F．研究発表

1．論文発表

1) Tohyama J, Akasaka N, Ohashi T, Kobayashi Y. Acquired opercular epilepsy with oromotor dysfunction: magnetoencephalographic analysis and efficacy of corticosteroid therapy. J Child Neurol 26: 885-890, 2011.

2) Yamazaki S, Ikeno K, Abe T, Tohyama J, Adachi Y. Hemiconvulsion-hemiplegia-epilepsy syndrome associated with *CACNA1A* S218L mutation. Pediatr Neurol 45: 193-196, 2011.

3) 大沢真木子，白坂幸義，大塚頌子，今井克美，御牧信義，佐々木征行，遠山　潤，赤坂紀幸，伊予田邦昭，山邊太陽，町井克行．日本人の小児難治てんかんの部分発作に対する gabapentin の併用療法の有効性と安全性の検討．臨床精神薬理．14:1205-1222, 2011.

2．学会発表

1)ヒョレア様の不随意運動をともなうWest症候群症例

遠山　潤，赤坂紀幸，大橋　伯，小林　悠，齋藤なか゛，熊田聡子，中川栄二，加藤光広
第53回日本小児神経学会総会　横浜

2) Involvement of chromosomal aberrations in patients with early epileptic encephalopathy.

Jun Tohyama, Hirotomo Saitsu, Keiko Shimojima, Noriyuki Akasaka, Tsukasa Ohashi, Yu Kobayashi, Toshiyuki Yamamoto, Naomichi Matsumoto, Mitsuhiro Kato.
第29回国際てんかん学会総会　ローマ

H．知的財産権の出願・登録状況

1．特許取得

なし．

2．実用新案登録

なし．

3．その他

なし．

別添4

研究成果の刊行に関する一覧表

書籍

著者氏名	論文タイトル名	書籍全体の編集者名	書　籍　名	出版社名	出版地	出版年	ページ
Shiraishi H.	Magnetoencephalography findings in medial temporal lobe epilepsy.	Felix Rosenow, Philippe Ryvlin and Hans Luders	The Mesial Temporal Lobe Epilepsies	John Libbey Eurotext	Surrey	2011	135-144

雑誌

発表者氏名	論文タイトル名	発表誌名	巻号	ページ	出版年
Nakamura K, Kato M, Sasaki A, Kanai M, Hayasaka K.	Congenital Dysplastic Microcephaly and Hypoplasia of the Brainstem and Cerebellum With Diffuse Intracranial Calcification.	J Child Neurol	doi: 10.1177/0883073811416239	Epub ahead of print	2012
Saitsu H, Igarashi N, Kato M, Okada I, Kosho T, Shimokawa O, Sasaki Y, Nishiyama K, Tsurusaki Y, Doi H, Miyake N, Harada N, Hayasaka K, Matsumoto N.	De novo 5q14.3 translocation 121.5-kb upstream of *MEF2C* in a patient with severe intellectual disability and early-onset epileptic encephalopathy.	Am J Med Genet	155A	2879-2884	2011
Kato M	Going BAC or oligo microarray to the well: a commentary on Clinical application of array-based comparative genomic hybridization by two-stage screening for 536 patients with mental retardation and multiple congenital anomalies.	J Hum Genet	56	104-105	2011
Tohyama J, Akasaka N, Ohashi T, Kobayashi Y.	Acquired opercular epilepsy with oromotor dysfunction: magnetoencephalographic analysis and efficacy of corticosteroid therapy.	J Child Neurol	26	885-890	2011

Tohyama J, Kato M, Kawasaki S, Harada N, Kawara H, Matsui T, Akasaka N, Ohashi T, Kobayashi Y, Matsumoto N.	Dandy-Walker malformation associated with heterozygous *ZIC1* and *ZIC4* deletion: Report of a new patient.	Am J Med Genet A	155A	130-133	2011
Yamazaki S, Ikeno K, Abe T, Tohyama J, Adachi Y.	Hemiconvulsion-hemiplegia-epilepsy syndrome associated with *CACNA1A* S218L mutation.	Pediatr Neurol	45	193-196	2011
Hirose M, Haginoya K, Yokoyama H, Kikuchi A, Hino-Fukuyo N, Munakata M, Uematsu M, Iinuma K, Kato M, Yamamoto T, Tsuchiya S.	Progressive atrophy of the cerebrum in 2 Japanese sisters with microcephaly with simplified gyri and enlarged extraaxial space.	Neuropediatrics	42	163-166	2011
Shiraishi H, Ahlfors SP, Stufflebeam SM, Knake S, Larsson PG, Hämäläinen MS, Takano K, Okajima M, Hatanaka K, Saitoh S, Dale AM, Halgren E.	Comparison of three methods for localizing interictal epileptiform discharges with magnetoencephalography.	J Clin Neurophysiol.	28	431-440	2011
Shiraishi H	Source localization in magnetoencephalography to identify epileptogenic foci.	Brain Dev.	33	276-281	2011
Yagyu K, Sueda K, Shiraishi H, Asahina N, Sakurai K, Kohsaka S, Sawamura Y, Saitoh S.	Direct correlation between the facial nerve nucleus and hemifacial seizures associated with a gangliocytoma of the floor of the fourth ventricle: A case report.	Epilepsia	52	e204-206	2011

Magnetoencephalograhpy findings in medial temporal lobe epilepsy

Hideaki Shiraishi

Department of Pediatrics, Hokkaido University School of Medicine, Japan

Magnetoencephalography (MEG) is a technique that arose from the superconductivity theory and is now applied to clinical investigations (Cohen *et al.*, 1968; Hamäläinen *et al.*, 1993). Studies of epileptic patients are a particularly useful application of MEG, because MEG provides better spatial and temporal resolution than electroencephalography (EEG).

Many reports have described the application of MEG for clinical investigations of epileptic patients (Knake *et al.*, 2004; Grondin *et al.*, 2006; Cappel *et al.*, 2006; Mäkelä *et al.*, 2006; Shibazaki *et al.*, 2007; Rampp *et al.*, 2007; Schwartz *et al.*, 2008). MEG currently plays an important role in the definition of the epileptogenic lesion in epileptic surgery candidates, especially those with neocortical epileptic lesions (Nakasato *et al.*, 1994; Sutherling *et al.*, 1987; Shiraishi *et al.*, 2001; Oishi *et al.*, 2006; Otsubo *et al.*, 2001; Otsubo *et al.*, 2005). By comparison, MEG analysis is more difficult when used to investigate medial temporal lobe epilepsy (MTLE), because the medial temporal structure is hidden anatomically in the depth of the temporal lobe (Shigeto *et al.*, 2002; Pataraia *et al.*, 2005). For this reason, the MEG current is not always detected because of the inherently low signal-to-noise ratio. In general, MEG can detect magnetic activity to a depth of less than 2 cm (Shigeto *et al.*, 2002). In this chapter, we describe the application of MEG for the diagnosis of MTLE in patients using specific analysis paradigms.

MEG source analysis

The MEG data are digitally filtered with a pass band of 3 to 30 Hz for offline analysis. Segments containing abnormal paroxysms are selected manually. Individual spikes aligned on the basis of the peak latency are analyzed. The distribution of brain activity generating the spikes is determined using two source estimation approaches: the equivalent current dipole (ECD) model and dynamic statistical parametric mapping (dSPM). The ECD model is appropriate when the underlying brain activity is focal, *i.e.* restricted to a relatively

small region of the brain. For non-focal brain activity, the distributed source models, including dSPM, are expected to be better suited than the ECD model for determining the distribution of brain activity generating the spikes.

Equivalent current dipoles

Equivalent current dipoles (ECDs) are calculated with the "xfit" software (Elekta-Neuromag Ltd.) using the single-dipole model. The conductivity geometry of the head is assumed to be spherically symmetrical. Dipoles are calculated for each time point measurement (every 2.5 ms) within a period of 100 ms at the vicinity of each MEG spike. All sensors are included in the analyses, with no selection of regions of interest. The initial location for the iterative fit of the ECD is chosen to be under the sensor with the largest signal. The ECD with the best goodness of fit (GOF) is selected as the representative ECD of that particular MEG spike. The GOF is a measure of how well the ECD model explains the measured signals. A dipole fit is accepted when the GOF is greater than 70%. To visualize anatomical locations, the ECDs are superimposed on the MRI from each patient.

Dynamic statistical parametric mapping

The dynamic statistical parametric mapping (dSPM) method (Dale et al., 2000) is based on a noise-normalized minimum L2-norm estimate. For dSPM analysis, we use an anatomically constrained, distributed source model, which assumes the sources are located in the cerebral cortex. The cortical surface is segmented from high-resolution MRI using the FreeSurfer software (Dale et al., 1999; Fischl et al., 1999) and subsampled to approximately 2500 elements per hemisphere. The source model consists of current dipole vectors located at each element. The forward solution is calculated using a boundary element method (BEM) model.

The dSPM approach used to estimate the time course of activity at each cortical location is based on the generalised least-squares or weighted minimum-norm solution (Hamäläinen, 1994; Dale, 1993); in this case, the estimate is normalized for noise sensitivity, thus providing a statistical parametric map (Dale et al., 2000). The noise normalization reduces the variation in the point-spread function between locations (Liu et al., 2002). Simulations have suggested that the spatial resolution is 15 mm or better (Dale et al., 2000; Liu et al., 2002). Maps are calculated at 2.5-ms intervals. The significance of modulation at each site is calculated using an F-test (Dale et al., 2000; Dhond et al., 2001). These statistical maps differ from maps of estimated source strengths, since the estimated noise variance is not constant across different cortical locations. However, since the same noise covariance estimates are used at all time points for given cortical locations, source strength at a given location over time is directly proportional to the statistical maps. The current approach provides dynamic statistical parametric maps of cortical activity, similar to the statistical maps typically generated using fMRI or PET data, but with a millisecond temporal resolution.

Short-time Fourier transform analysis

Short-time Fourier transform (STFT) analysis is used to reveal the distributions of MEG polyspikes (Oppenheim et al., 1999). The MATLAB (MathWorks, Natick, MA, USA) program is used to execute the STFT for the MEG signals. Each signal is divided into small sequential frames, and fast Fourier transformation (FFT) is applied to each frame.

In the present study, the STFT was implemented using a 256-point window. The time of each window was 426.7 ms (*i.e.* 256 points × 1,000 ms/600 Hz). The window was shifted every four points, which corresponded to 6.7 ms (*i.e.* 1,000 ms/600 Hz × 4 points). FFT was applied to each window. This process was repeated for all selected signals. The time-frequency distributions are displayed as graphs.

Fourier transform is performed with frequencies in the ranges of 3-30 Hz, 30-50 Hz, and 50-100 Hz. A spectrum is considered to be aberrant when it is observed to be isolated from the background frequency spectrum in the graph. An aberrant frequency spectrum on the graph is superimposed onto the reconstructed 3D-MRI.

Electrocortigogram

An electrocorticogram (ECoG) study is performed during surgery. The ECoG data are collected using the Ceegraph system (Bio-Logic, Mundelein, IL, USA), with a sampling rate of 512 Hz. A 4 × 5 grid electrode array was used in the second case report. The recording is performed for at least one minute at each electrode location.

Case report 1

We report the case of a 17-year-old girl. Her epilepsy started when she was 11 years old with simple partial seizures described as cephalic sensation, and complex partial seizures described as motion arrest, oral automatism, and bilateral manual automatisms lasting for 2-3 minutes without dystonic posturing or secondary generalised tonic-clonic seizures (GTCs). Over time, her seizures had become more frequent and occurred more than once per week.

She had a selective amygdala-hippocampectomy at 15 years of age and has been seizure-free for three years (Engel class I).

EEG, MEG, MRI, SPECT, and PET findings are shown in *Figure 1*. Her spike sources were localized by ECDs at the pole and base of the left temporal lobe. The location and distribution of her ECDs were consistent with the typical location and distribution of the horizontal ECD described in MTLE (Stefan *et al.*, 2003). ECDs are not always located at the hippocampus, but may be located at other areas of the temporal lobe. It is not always possible to detect MEG activity because of the low signal-to-noise ratio.

Case report 2

We report the case of a nine-year-old girl. Her epilepsy started at one month of age with complex partial seizures with motion arrest and cyanosis. Her seizures evolved to daily simple partial seizures, described as ictal fear and cephalic sensations, and complex partial seizures with motion arrest and autonomic change (cyanotic face) for three to four minutes without dystonic posturing.

At the age of nine years she underwent resection of focal cortical dysplasia at the medial aspect of the left temporal lobe and the head of the hippocampus. She has now been seizure-free for one year and eight months. Initial EEG and MEG measurements showed no epileptiform discharges *(Figure 2A)*. Sequential EEG and MEG measurements demonstrated activity in the right occipital and left frontal areas, but not to the same level of activity recorded from the left temporal area, where the focal cortical dysplasia was located

(*Figure 2B*). Furthermore, EEG and MEG measurements showed intermittent, but prolonged rhythmic activity in the left frontal and temporal region (*Figure 2B*). This rhythmic activity was no longer observed after her operation (*Figure 2C*).
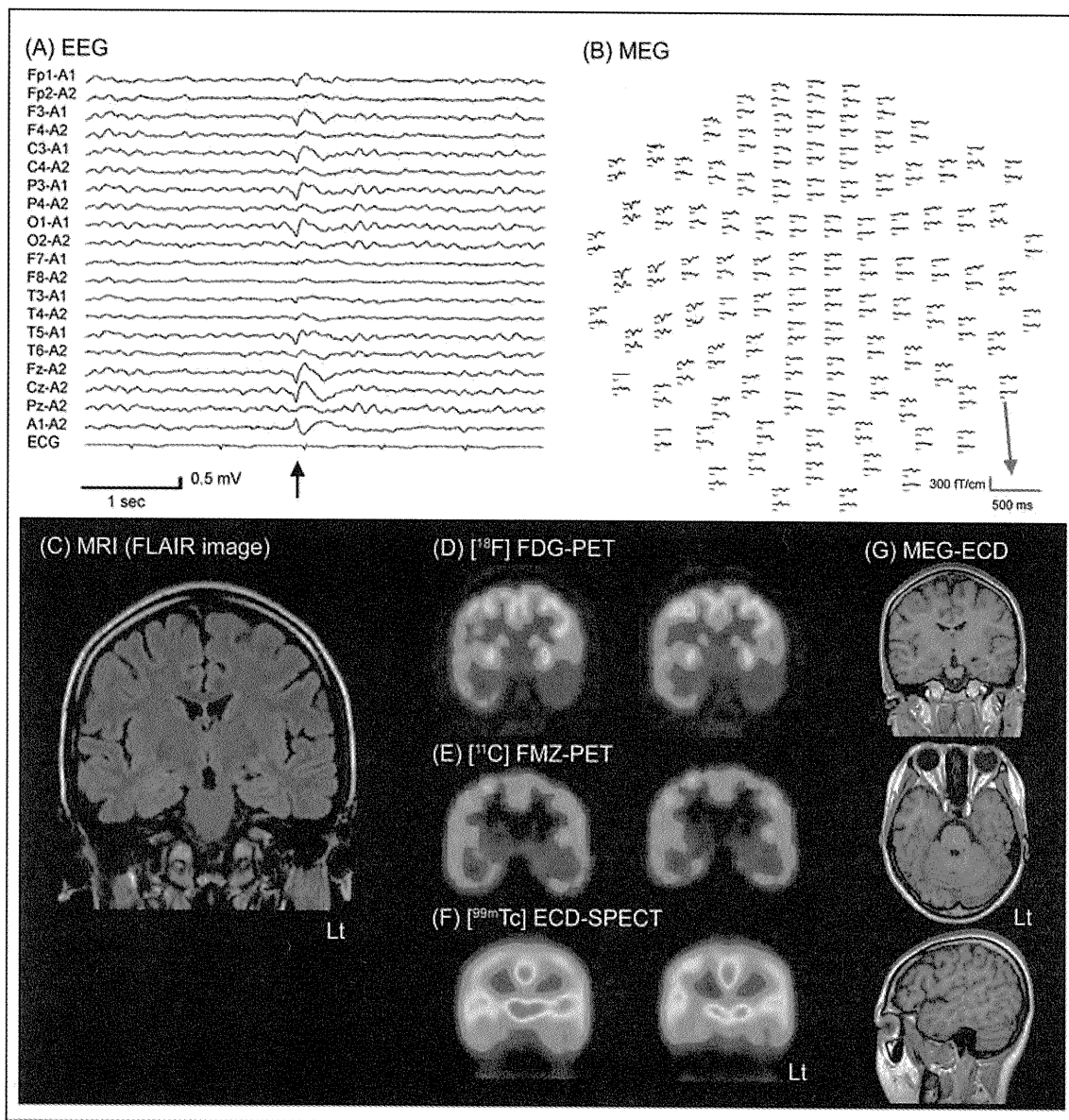
Figure 1. Case 1: EEG, MEG, MRI, PET and interictal SPECT.
A) EEG showing left hemispheric positive spikes which were reflected by the epileptic current at reference electrode A1. **B)** MEG showing spikes in the left temporal region. **C)** MRI showing atrophy and sclerosis of the left hippocampus of the patient. **D)** [^{18}F] Fluorodeoxyglucose (FDG) positron emission CT (PET) showing hypometabolism in the left medial temporal lobe. **E)** [^{11}C] Flumazenil (FMZ) PET showing low benzodiazepine receptor binding in the left medial temporal lobe. **F)** Interictal [^{99m}Tc] ethylcysteinate dimer (ECD) single photon emission CT (SPECT) showing low perfusion in left medial temporal structures. **G)** The location of MEG ECDs of epileptiform activity were located at the pole and base of the left temporal lobe in a horizontal direction.
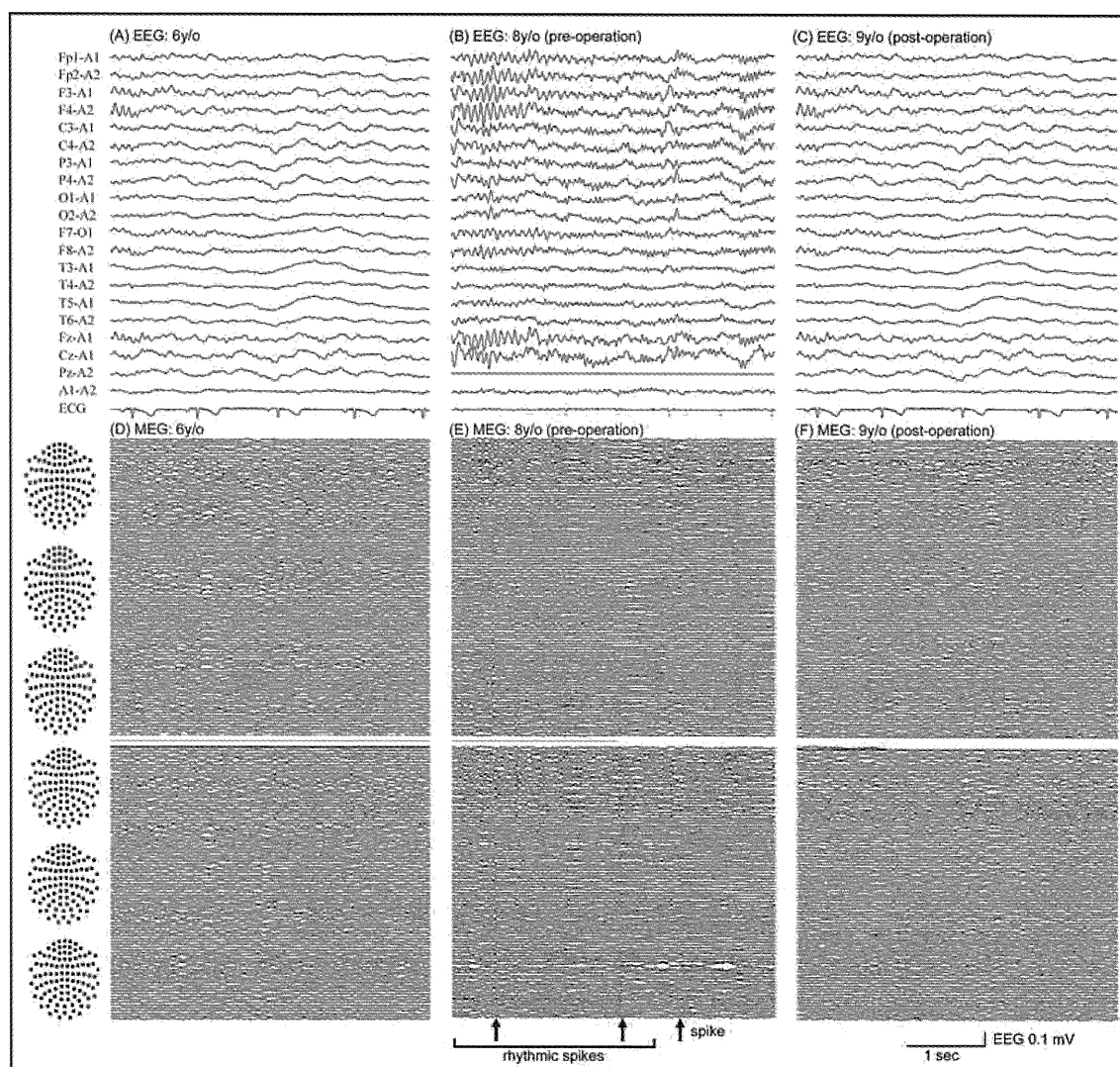
Figure 2. Case 2: EEG and MEG.
A) EEG at six years of age on her first visit showing no epileptiform discharges. **B)** EEG at eight years of age just before her operation showing prolonged rhythmic spiking with 10 Hz oscillation at Fp1, Fp2, F3, F4, F7, F8 and Fz. Independent spikes were detected at Fp1, Fp2, F3, C3, P3, P4, O1, O2 and Cz. **C)** EEG at nine years of age after her operation showing fragmental rhythmic activities at F3, F4 F7, F8 and Fz. **D)** MEG at six years of age on her first visit showing no epileptiform discharge. **E)** MEG at eight years of age just before her operation showing continuous aberrant oscillation at approximately 20 Hz at the left frontal area and the occipito-parietal area (quoted). MEG shows the frequent occurrence of an independent spike at the right occipital area and the left frontal area (arrow). **F)** MEG at nine years of age after her operation showing a spatially restricted oscillation band at the left frontal area at approximately 16 Hz.

To investigate the widespread spikes in MEG just before the operation, ECDs were located at the left superior frontal gyrus and the right supra-marginal gyrus (*Figure 3B*). dSPM analysis revealed genesis of the spikes at the right supra-marginal gyrus and propagation to left superior frontal gyrus and medial aspect (*Figure 3C*). In this situation, the ECD measurements only represented propagation of activity from a distinct epileptogenic area.
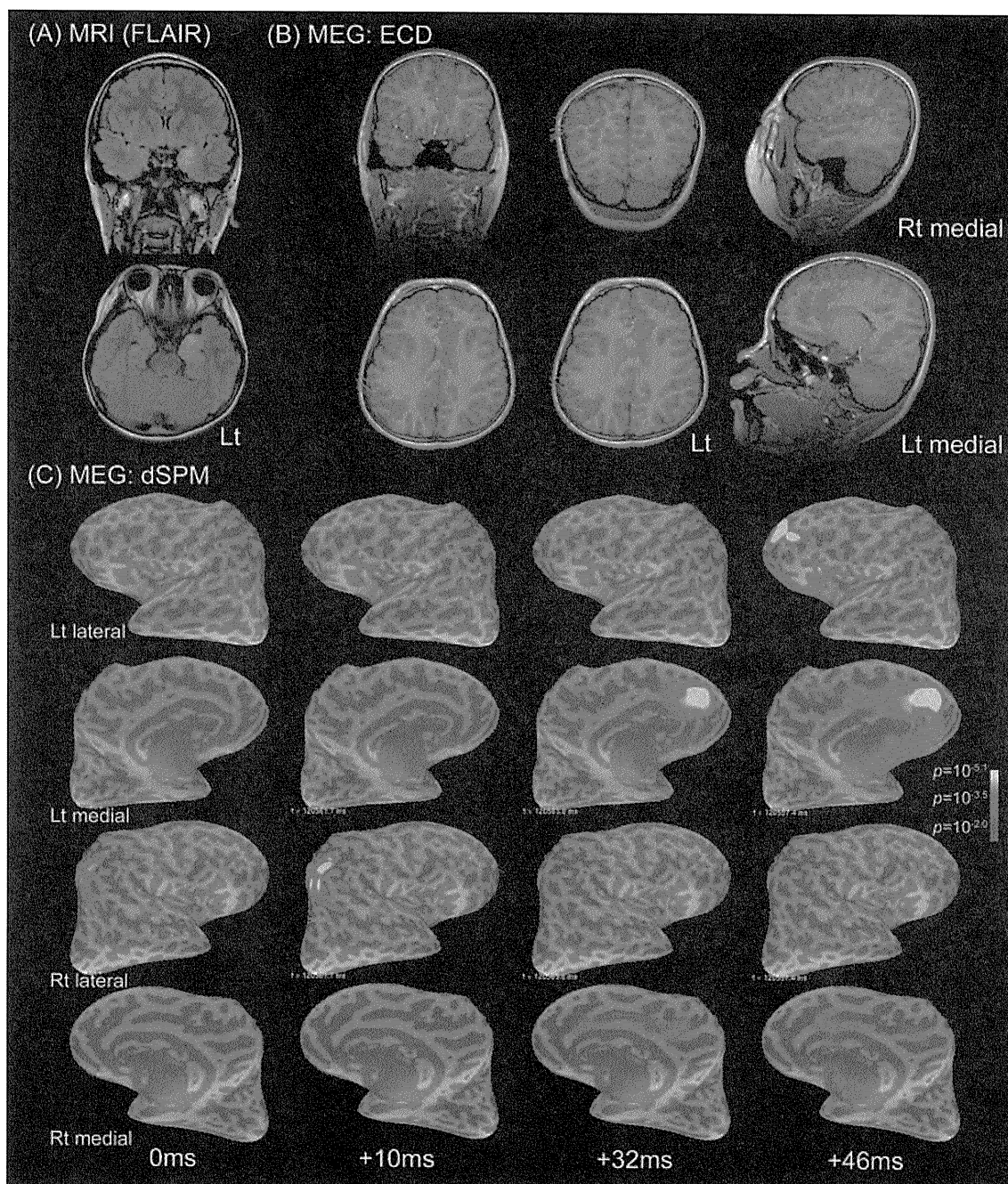
Figure 3. Case 2: MRI and MEG.
A) MRI FLAIR images showing focal cortical dysplasia at the left temporal para-hippocampal gyrus, uncus and hip-pocampus. **B)** ECDs were located at the left superior frontal gyrus and the right supra-marginal gyrus. **C)** dSPM snapshots demonstrated epileptiform activity generated in the right supra-marginal gyrus, which propagated to the left superior frontal gyrus and the corresponding medial aspect. In inflated MRI, dark and light grey areas revealed the sulcus and gyrus, respectively. The area in yellow, the point of transition from red to yellow, and the point of transition from grey to red, represent statistical values with p = $10^{-5.1}$, $10^{-3.5}$, and $10^{-2.0}$, respectively.

She underwent SFT analysis for preoperative and postoperative rhythmic activity (*Figure 4A, 4C*). SFT analyses demonstrated rhythmic activity in the ipsilateral frontal lobe and within a broad region of the lateral aspect of the temporal lobe (*Figure 4B*). After the operation these rhythmic activities disappeared and became localized to the left pre- and post-central gyrus (*Figure 4D*).
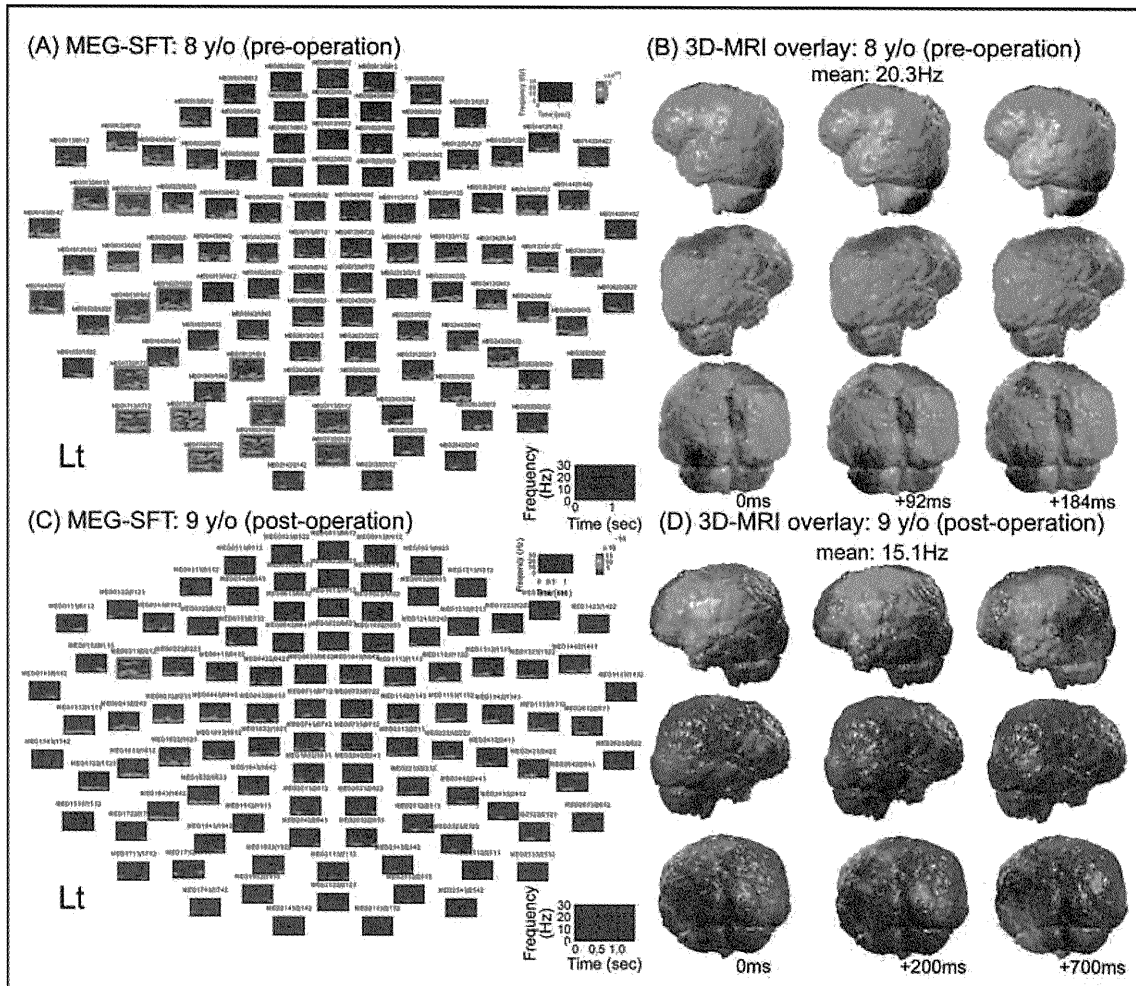

Figure 4. Case 2: STFT analysis.

A) STFT at eight years of age just before her operation showed aberrant magnetological oscillation at the left occipital and temporal and frontal areas at approximately 20 Hz (surrounded by red lines). **B)** EG signal from (**A**), superimposed on the 3D MRI image showing broad aberrant oscillation in the left lateral occipital lobe, the inferior, middle, and superior temporal gyrus, the angular gyrus, the supra-marginal gyrus and the inferior frontal gyrus (red and yellow areas). **C)** STFT at nine years of age after her operation showing aberrant magnetic field oscillation in the left frontal region at approximately 20 Hz (surrounded by red lines). **D)** MEG signal from (**C**), superimposed on the 3D MRI image showing broad aberrant oscillation in the left angular gyrus and the inferior frontal gyrus (red and yellow area).

She underwent ECoG during the operation. Just before the dysplasia resection, continuous rhythmic spikes at approximately 20 Hz were detected at the lower area of the left pre- and post-central gyrus and supra-marginal gyrus (*Figure 5A*). This activity disappeared and the irritative zone became more restricted to the left pre-frontal gyrus and supra-marginal

gyrus from where epileptiform activity with lower amplitude was now recorded (*Figure 5B*). These findings provide clear evidence of the power reduction of the irritative zone after surgery.
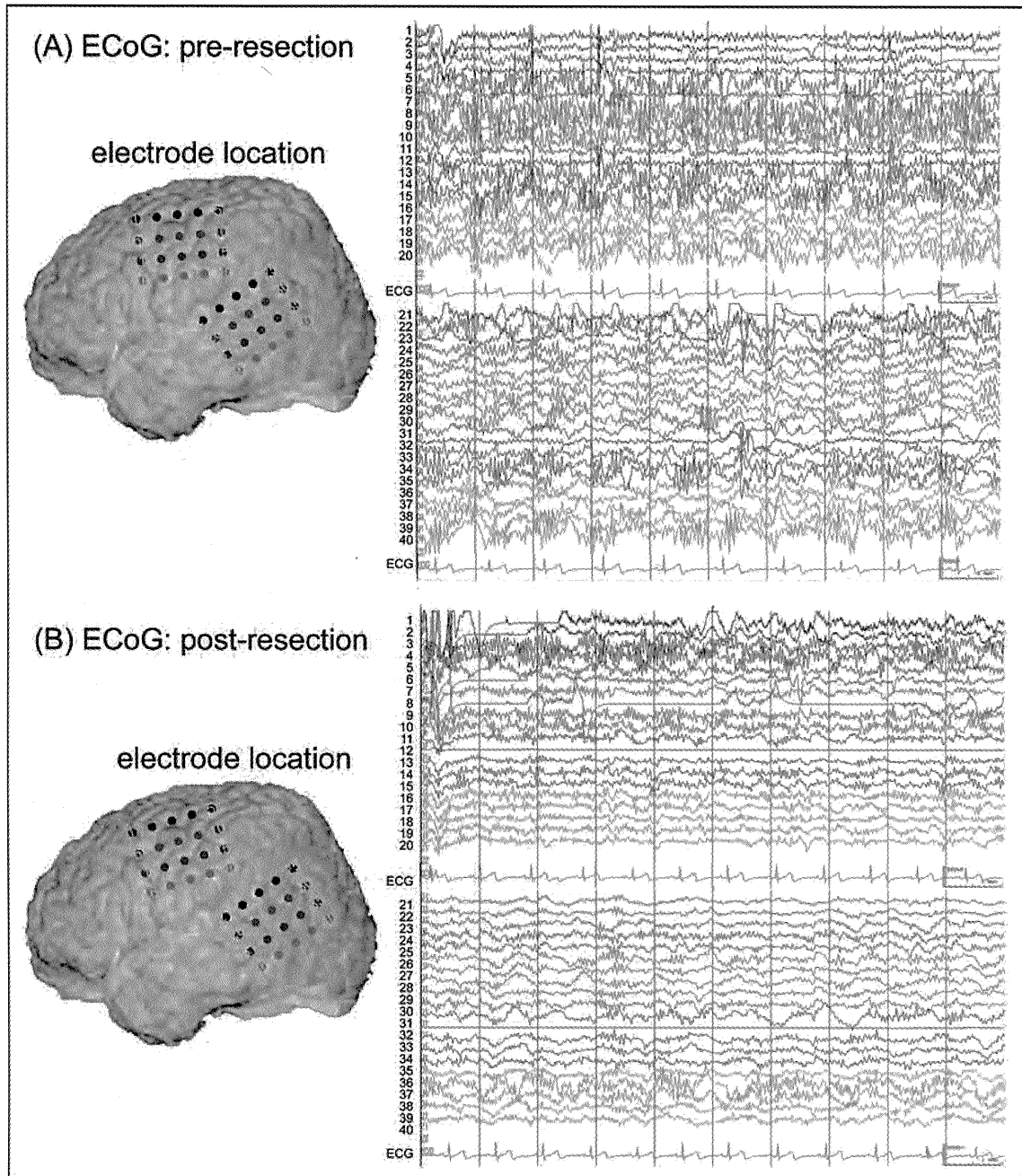
Figure 5. Case 2: ECoG.
A) ECoG during the operation before resection of the lesion demonstrating continuous aberrant rhythmic discharges at 20 Hz in electrode 5, 6, 7, 8, 9, 10, 13, 14, 15, 28, 19, 33, 34, 39 and 10 at approximately 500 μV. **B)** ECoG during the operation after resection of the lesion demonstrating an aberrant oscillation area at electrode 3, 4, 9, 10, 37 and 38 at approximately 250 μV.

▪ Discussion and conclusion

MEG analysis is not the optimal tool for the identification of the epileptogenic area in patients with MTLE. MEG is reported to detect only about 50% of the ECoG spikes generated from medial temporal structures (Shigeto et al., 2002; Pataraia et al., 2005). However, a seizure-free (Engel class I) outcome was achieved in more than 90% of the patients after epilepsy surgery when the results using the ECD model showed horizontal currents from the ipsilateral medial temporal lobe (Assafa et al., 2004). Furthermore, in patients with medial temporal sclerosis (MTS) on MRI and a definite history of complex partial seizures (CPS), negative MEG findings provide further evidence that MTLE patients are good surgical candidates.

In this chapter, the investigation of epileptic rhythmic activity by MEG, which may reveal the presence of widespread aberrant epileptic discharges from medial temporal structures, was discussed. For follow-up evaluation in MTLE patients who have undergone surgery, MEG holds the potential to non-invasively grade the propensity for seizure recurrence. At this stage, the evidence highlights the potential of MEG as a valuable non-invasive tool before and after surgery for sequential evaluation, especially in paediatric patients.

References

- Assafa BA, Karkarb KM, Laxerc KD, Garciab PA, Austin EJ, Nicholas M, et al. Magnetoencephalography source localization and surgical outcome in temporal lobe epilepsy. Clin Neurophysiol 2004; 115: 2066-76.

- Cappell J, Schevon C, Emerson RG. Magnetoencephalography in epilepsy: tailoring interpretation and making inferences. Curr Neurol Neurosci Rep 2006; 6: 327-31.

- Cohen D. Magnetoencephalography: evidence of magnetic fields produced by alpha-rhythm currents. Science 1968; 161: 784-6.

- Dale AM, Fischl B, Sereno MI. Cortical surface-based analysis. I. Segmentation and surface reconstruction. Neuroimage 1999; 9: 179-94.

- Dale AM, Liu AK, Fischl BR, Buckner RL, Belliveau JW, Lewine JD, et al. Dynamic statistical parametric mapping: combining fMRI and MEG for high-resolution imaging of cortical activity. Neuron 2000; 26: 55-67.

- Dale AM, Sereno MI. Improved localization of cortical activity by combining EEG and MEG with MRI cortical surface reconstruction: A linear approach. J Cogn Neurosci 1993; 5: 162-76.

- Dhond RP, Buckner RL, Dale AM, Marinkovic KM, Halgren E. Spatiotemporal maps of brain activity underlying word generation and their modification during repetition priming. J Neurosci 2001; 21: 3564-71.

- Fischl B, Sereno MI, Tootell RB, Dale AM. High-resolution intersubject averaging and a coordinate system for the cortical surface, Hum Brain Mapp 1999; 8: 272-84.

- Grondin R, Chuang S, Otsubo H, Holowka S, Snead OC 3rd, Raybaud C, et al. The role of magnetoencephalography in pediatric epilepsy surgery. Childs Nerv Syst 2006; 22: 779-85.

- Hamäläinen M, Hari R, Ilmoniemi RJ, Knuutila J, Lounasmaa OV. Magnetoencephalography: theory, instrumentation, and application to noninvasive studies of the working human brain. Rev Mod Phys 1993; 65: 413-97.

- Hamäläinen MS, Ilmoniemi RJ. Interpreting magnetic fields of the brain: minimum norm estimates. Med Biol Eng Compu 1994; 32: 35-42.

- Knake S, Grant PE, Stufflebeam SM, Wald LL, Shiraishi H, Rosenow F, et al. Aids to telemetry in the presurgical evaluation of epilepsy patients: MRI, MEG and other non-invasive imaging techniques. Suppl Clin Neurophysiol 2004; 57: 494-502.

- Liu AK, Dale AM, Belliveau JW. Monte Carlo simulation studies of EEG and MEG localization accuracy. Hum Brain Mapp 2002; 16: 47-62.

- Mäkelä JP, Forss N, Jääskeläinen J, Kirveskari E, Korvenoja A, Paetau R. Magnetoencephalography in neurosurgery. Neurosurgery. 2006; 59: 493-510; 510-1.

- Nakasato N, Levesque MF, Barth DS, Baumgartner C, Rogers RL, Sutherling WW. Comparisons of MEG, EEG, and ECoG source localization in neocortical partial epilepsy in humans. Electroencephalogr Clin Neurophysiol 1994; 91: 171-8.

- Oishi M, Kameyama S, Masuda H, Tohyama J, Kanazawa O, Sasagawa M, et al. Single and multiple clusters of magnetoencephalographic dipoles in neocortical epilepsy: Significance in characterizing the epileptogenic zone. Epilepsia 2006; 47: 355-64.

- Oppenheim A, Schafer RW. Discrete-Time Signal Processing. Englewood Cliffs: Prentice Hall, 1999.

- Otsubo H, Ochi A, Elliott I, Chuang SH, Rutka JT, Jay V, et al. MEG predicts epileptic zone in lesional extrahippocampal epilepsy: 12 pediatric surgery cases. Epilepsia 2001; 42: 1523-30.

- Otsubo H, Iida K, Okuda C, Ochi A, Pang E, Weiss SK, et al. Neurophysiological findings of neuronal migration disorders: intrinsic epileptogenicity of focal cortical dysplasia on EEG, ECoG, and MEG. J Child Neurol 2005; 20: 357-63.

- Pataraia E, Lindinger G, Deecke L, Mayer D, Baumgartner C. Combined MEG/EEG analysis of the interictal spike complex in mesial temporal lobe epilepsy. Neuroimage 2005; 24: 607-14.

- Rampp S, Stefan H. Magnetoencephalography in presurgical epilepsy diagnosis. Expert Rev Med Devices 2007; 4: 335-47.

- Schwartz ES, Dlugos DJ, Storm PB, Dell J, Magee R, Flynn TP, et al. Magnetoencephalography for pediatric epilepsy: how we do it. AJNR Am J Neuroradiol 2008; 29: 832-7.

- Shibasaki H, Ikeda A, Nagamine T. Use of magnetoencephalography in the presurgical evaluation of epilepsy patients. Clin Neurophysiol 2007; 118: 1438-48.

- Shigeto H, Morioka T, Hisada K, Nishio S, Ishibashi H, Kira D, et al. Feasibility and limitations of magnetoencephalographic detection of epileptic discharges: simultaneous recording of magnetic fields and electrocorticography. Neurol Res 2002; 24: 531-6.

- Shiraishi H, Watanabe Y, Watanabe M, Inoue Y, Fujiwara T, Yagi K. Interictal and ictal magnetoencephalographic study in patients with medial frontal lobe epilepsy. Epilepsia 2001; 42: 875-82.

- Stefan H, Hummel C, Scheler G, Genow A, Druschky K, Tilz C, et al. Magnetic brain source imaging of focal epileptic activity: a synopsis of 455 cases. Brain 2003; 126: 2396-405.

- Sutherling WW, Crandall PH, Engel J Jr, Darcey TM, Cahan LD, Barth DS. The magnetic field of complex partial seizure agrees with intracranial localizations. Ann Neurol 1987; 21: 548-58.

Congenital Dysplastic Microcephaly and Hypoplasia of the Brainstem and Cerebellum With Diffuse Intracranial Calcification

Kazuyuki Nakamura, MD, Mitsuhiro Kato, MD, PhD,
Ayako Sasaki, MD, PhD, Masayo Kanai, MD, PhD, and
Kiyoshi Hayasaka, MD, PhD

Abstract

Congenital microcephaly with intracranial calcification is a rare condition presented in heterogeneous diseases. Here, we report the case of a 1-year-old boy with severe congenital microcephaly and diffuse calcification. Neuroimaging studies showed a diffuse simplified gyral pattern; a very thin cortex; ventricular dilatation; very small basal ganglia, thalamus, and brainstem; and cerebellar hypoplasia with diffuse calcification. Clinical features of intrauterine infections, such as neonatal jaundice, hepatomegaly, and thrombocytopenia, were not found. Serological tests, cultures, and polymerase chain reaction analysis were negative for viral infections. The etiology of pseudo–toxoplasmosis, rubella, cytomegalovirus, and herpes simplex syndrome is still unknown. This study describes the most severe form of pseudo–toxoplasmosis, rubella, cytomegalovirus, and herpes simplex syndrome reported to date, with the patient showing microcephaly and calcification or band-like intracranial calcification with simplified gyration and polymirogyria.

Keywords

microcephaly, intracranial calcification, pontocerebellar hypoplasia, toxoplasmosis, rubella, cytomegalovirus, herpes simplex

Congenital microcephaly with brain dysgenesis and intracranial calcification is a characteristic feature of intrauterine infections of toxoplasma, rubella, cytomegalovirus, herpes virus, and other infectious agents, including human immunodeficiency virus and the bacteria that cause syphilis. This form of congenital microcephaly has been termed the toxoplasmosis, rubella, cytomegalovirus, and herpes simplex syndrome.[1] In addition to congenital microcephaly and intracranial calcification, toxoplasmosis, rubella, cytomegalovirus, and herpes simplex syndrome shows systemic abnormalities, such as thrombocytopenia, anemia, hepatosplenomegaly, liver dysfunction, jaundice, and chorioretinitis, with elevated serum immunoglobulin M (IgM) levels at birth. Similar clinical conditions have been reported in several patients with familial occurrence but with no evidence of infection. These clinical conditions have been designated as "pseudo–toxoplasmosis, rubella, cytomegalovirus, and herpes simplex" syndrome.[2] In addition, "band-like intracranial calcification with simplified gyration and polymicrogyria" has also been reported. However, this syndrome shows no evidence of infection, abnormalities in liver function, or thrombocytopenia.[3,4]

It is important to discriminate these syndromes for genetic counseling. This report describes a patient with congenital microcephaly and whole brain dysgenesis and extensive calcification, suggesting a severe form of pseudo–toxoplasmosis, rubella, cytomegalovirus, and herpes simplex syndrome, or band-like intracranial calcification with simplified gyration and polymicrogyria.

Case Report

The boy was born to healthy, unrelated, 29-year-old Japanese parents. This was the mother's first pregnancy, and the boy had no siblings. There were no household pets including cats. During the 5- to 6-week period of gestation, his mother had fever for 1 day but showed no other symptoms. Microcephaly was first observed on ultrasound examination conducted at 28 weeks of gestation. At 34 weeks of gestation, specific IgMs

Department of Pediatrics, Yamagata University Faculty of Medicine, Yamagata, Japan

Corresponding Author:
Kazuyuki Nakamura, MD, Department of Pediatrics, Yamagata University Faculty of Medicine, 2-2-2, Iida-Nishi, Yamagata 990-9585, Japan
Email: kazun-yamagata@umin.ac.jp
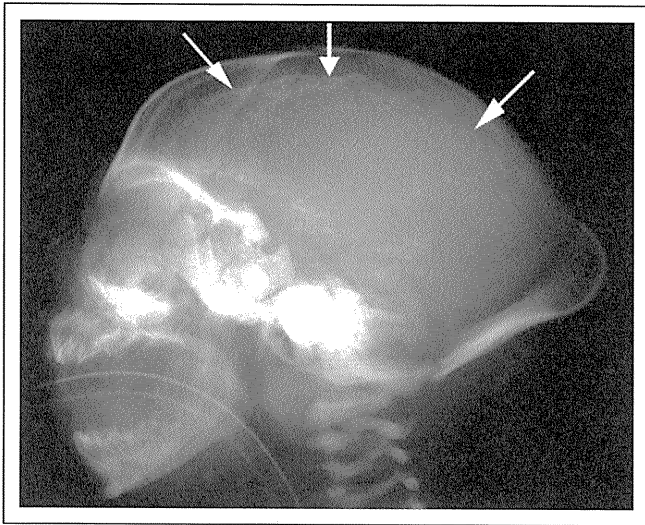
Figure 1. A plain radiograph of the head shows the cranial vault with a frontal sloping and a marked external occipital protuberance. Intracranial high-density spots are visible along the cerebral wall (arrows).

against rubella, cytomegalovirus, and toxoplasma were negative in the mother. He was delivered by caesarean section because of hypotonic uterine dysfunction at 42 weeks of gestation. His Apgar score was 1 at 1 min. He required intratracheal intubation for severe dyspnea. His weight at birth was 3140 g; length, 46 cm (−2.0 SD); and head circumference, 29 cm (−3.2 SD). He had bilateral undescended testis without hepatosplenomegaly or a petechial rash. Ophthalmologic examination showed no corneal clouding or chorioretinitis. Neurological examination showed the presence of hypotonic muscles and absence of a Moro reflex. Skull radiography showed a sloping forehead and several intracranial calcific densities (Fig. 1). A computed tomographic (CT) scan of the head showed prominent calcification mainly along the ventricular wall from the cerebrum to the brain stem (Fig. 2). Magnetic resonance imaging (MRI) of the brain showed severe diffuse simplified gyri combined with a thinning of the cortex and the white matter; marked dilated ventricles; and severe hypoplasia of the basal ganglia, thalamus, cerebellum, and brainstem (Fig. 3). At the age of 4 days, a hematological examination (hemoglobin, 18.3 g/dL; white blood cells, 10 010/μL; neutrophils, 69%; platelets, 32.8 × 10^4/μL^3) and blood chemistry tests, including those for calcium, phosphate, aspartate aminotransferase, alanine aminotransferase, lactate, and amino acids were normal. The total serum IgM was 8 mg/dL; the specific IgMs against toxoplasma, rubella, cytomegalovirus, herpes simplex, and varicella-zoster virus were negative. Viral cultures of a pharyngeal swab and urine were negative. Subsequent polymerase chain reaction (PCR) amplification of cytomegalovirus DNA in urine and the umbilical cord was also negative. An antibody titer for lymphocytic choriomeningitis virus was negative. G-banding chromosomal analysis showed a karyotype of 46, XY. At the age of 10 months, a cerebrospinal fluid examination did not show increased number of lymphocytes or interferon-alpha.
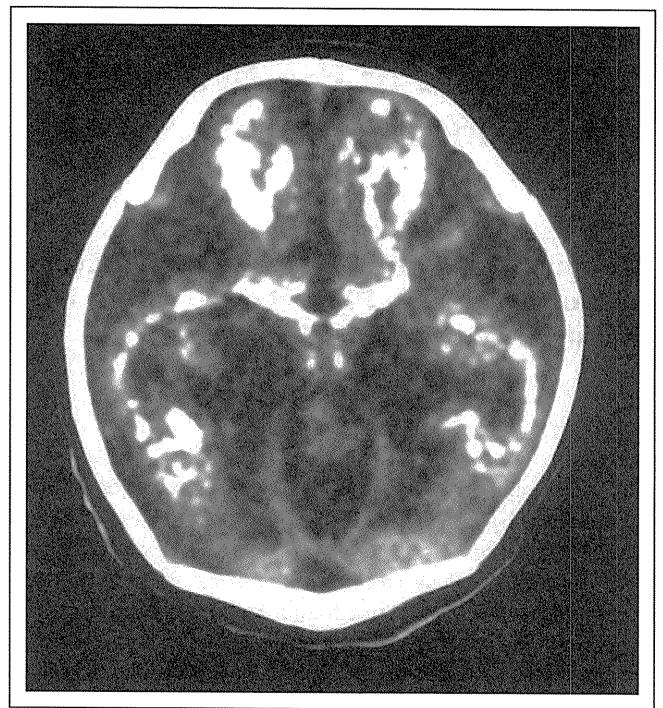

Figure 2. Computed tomographic scan of the head shows linear or patchy high signals consisting of calcifications within or immediately beneath the cortex and the enlargement of the lateral ventricles.

Electroencephalography showed multifocal sharp waves with low-voltage background activity. At 12 months of age, he showed hypothermia (<36°C); recurrent urinary tract infections caused by vesicoureteral reflux; and a profound developmental delay with limb contractures, no eye contact, and no head control. He received tube feeding because of bulbar palsy.

Discussion

Congenital microcephaly results from various clinical conditions such as infections, radiation, exogenous toxic agents, anoxic or metabolic insults, and genetic bases.[1] Although these conditions can also cause cerebral calcification, the association of congenital microcephaly and calcification are rare. Our patient experienced a febrile episode, suggesting an infection at 5 to 6 weeks of gestation, but there was no history of any other insult. Since intrauterine infections or toxoplasmosis, rubella, cytomegalovirus, and herpes simplex syndrome, especially cytomegalovirus infection, is the most frequent cause of congenital microcephaly and since calcification and earlier infection induce severer brain anomalies,[1] we tried to obtain evidence of a prenatal infection of cytomegalovirus using serological tests, cultures, and PCR amplification. However, none of these tests yielded a positive result, which could be a result of early infection during fetal development. The fetus showed no immunological response, and the virus could not be cultured. Moreover, the PCR sensitivity was sufficiently high enough to detect viral DNA.[5] On
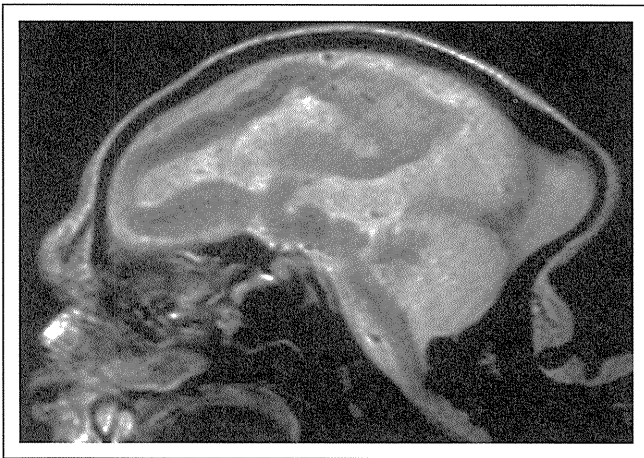
Figure 3. Sagittal T2-weighted magnetic resonance imaging (MRI) shows a thin cortex and white matter with an undetectable border. Prominent hypoplasia of the cerebellum and brainstem is visible.

the basis of these results, we conclude that cytomegalovirus is unlikely to be the cause of our patient's condition.

During the middle embryonic period (5–6 weeks of gestation in humans), secondary brain vesicles (telencephalon, diencephalon, mesencephalon, metencephalon, and myelencephalon) are formed; the primitive cerebral hemispheres develop during neuronogenesis in the ventricular zone. Insult at this stage can engender extremely severe brain malformation (eg, decreased brain size) because of the inhibition of cell proliferation and the dysplastic configuration of the brain that results from impaired cell migration. The hypoplastic brainstem and cerebellum as well as microcephaly with the thin cortex and irregular convolution seen in our patient suggest an event during early embryogenesis, although the etiology is unknown.

Although our patient showed an irregular convolution that suggested possible cortical dysplasia, the very thin cortex suggested microcephaly with normal to thin cortex or microcephaly with a simplified gyral pattern.[6] To date, 5 genes (*MCPH1, ASPM, CDK5RAP2, CENPJ,* and *SLC25A19*) have been found to be responsible for the autosomal recessive inheritance of microcephaly with a simplified gyral pattern.[7,8] Mutations in these genes result in congenital microcephaly but not in a calcification resembling the one in our patient. Microcephaly with polymicrogyria or other cortical dysplasias or microcephaly with pontocerebellar hypoplasia are other candidate conditions for our patient, but neither one shows calcification.[9] At this point, it is difficult to categorize the neuroimaging features of our patient into the classification scheme for malformations of cortical development.[6]

Aicardi–Goutières syndrome is an autosomal recessive form of progressive encephalopathy characterized by acquired microcephaly, leukodystrophy, and calcifications of the basal ganglia, which is similar to toxoplasmosis, rubella, cytomegalovirus, and herpes simplex syndrome.[10] Recently, 5 genes (*TREX1, RNASEH2B, RNASEH2C, RNASEH2A,* and *SAMHD1*) have been identified as the responsible genes for this syndrome.[11-13] Elevated interferon-alpha levels and chronic

lymphocytosis in the cerebrospinal fluid are specific features of Aicardi–Goutières syndrome. However, our patient had neither of these features. Although cerebrospinal fluid lymphocytosis is not necessary for an Aicardi–Goutières syndrome diagnosis[14] and although a small number of patients show microcephaly at birth, the cerebral dysplasia observed in our patient has never been reported as a manifestation of Aicardi–Goutières syndrome.

It has been suggested that pseudo–toxoplasmosis, rubella, cytomegalovirus, and herpes simplex syndrome is the same disorder as Aicardi–Goutières syndrome.[15] Periventricular areas are commonly calcified in pseudo–toxoplasmosis, rubella, cytomegalovirus, and herpes simplex syndrome, but the basal ganglia, cerebellum, and brainstem can also be affected. Brain MRIs often show cerebral atrophy, enlarged lateral ventricles, and severe hypoplasia of the corpus callosum, cerebellum, and brainstem. Some patients also show associated cortical dysplasia.[2,16] One report described a patient as having microcephaly with plate-like cortical calcification and with an extremely decreased convolution of the cerebral cortex, which is similar to our patient's condition.[17] However, the brainstem and cerebellum were spared in that patient.

Band-like intracranial calcification with simplified gyration and polymicrogyria is inherited as an autosomal recessive trait, and mutations of the *OCLN* gene have been identified as resulting in this condition.[18] Band-like intracranial calcification with simplified gyration and polymicrogyria is similar to pseudo–toxoplasmosis, rubella, cytomegalovirus, and herpes simplex syndrome in that both show widespread intracranial calcification and polymicrogyria and that some patients show hypoplasia of the cerebellum and brainstem. There are differences between these 2 conditions in terms of the postnatal microcephaly, the characteristic band-like calcification, and the lack of evidence for neonatal disturbance of liver function with thrombocytopenia; nonetheless, they can have similar etiologies.[3,4]

The extensive lesions of the brain are reminiscent of multicystic encephalomalacia, which are often accompanied by extensive dystrophic calcifications in zones of infarction. Multicystic encephalomalacia is also caused by fetal viral infection as well as hypoxia or circulatory insults; however, the lesions in the patient appeared to be too broad for secondary injury and had no visible cysts, as observed by MRI. The size and number of cysts depends on the stage of infarction, which can be both of major cerebral vessels and of the microcirculation at capillary levels.[19] Neuropathological confirmation is essential to reveal the pathogenesis.

It is noteworthy that this is the most severe case of a patient with congenital dysplastic microcephaly and brainstem and cerebellar hypoplasia with extensive intracranial calcification. The pathogenesis, particularly regarding its inheritance, remains to be clarified.

Acknowledgments

Author Contributions

Declaration of Conflicting Interests

Funding

Ethical Approval

References

1. Volpe JJ. In: *Neurology of the Newborn*. 5th ed. Philadelphia, PA: WB Saunders;; 2008.
2. Vivarelli R, Grosso S, Cioni M, et al. Pseudo-TORCH syndrome or Baraitser-Reardon syndrome: diagnostic criteria. *Brain Dev*. 2001;23:18-23.
3. Briggs TA, Wolf NI, D'Arrigo S, et al. Band-like intracranial calcification with simplified gyration and polymicrogyria: a distinct "pseudo-TORCH" phenotype. *Am J Med Genet A*. 2008;146: 3173-3180.
4. Abdel-Salam GM, Zaki MS, Saleem SN, Gaber KR. Microcephaly, malformation of brain development and intracranial calcification in sibs: pseudo-TORCH or a new syndrome. *Am J Med Genet A*. 2008;146:2929-2936.
5. Revello MG, Zavattoni M, Furione M, et al. Diagnosis and outcome of preconceptional and periconceptional primary human cytomegalovirus infections. *J Infect Dis*. 2002;186:553-557.
6. Barkovich AJ, Kuzniecky RI, Jackson GD, et al. A development and genetic classification for malformations of cortical development. *Neurology*. 2005;65:1873-1887.
7. Rosenberg MJ, Agarwala R, Bouffard G, et al. Mutant deoxynucleotide carrier is associated with congenital microcephaly. *Nat Genet*. 2002;32:175-179.
8. Woods CG, Bond J, Enard W. Autosomal recessive primary microcephaly (MCPH): a review of clinical, molecular, evolutionary findings. *Am J Hum Genet*. 2005;76:717-728.
9. Hashimoto K, Takeuchi Y, Kida Y, et al. Three siblings of fatal infantile encephalopathy with olivopontocerebellar hypoplasia and microcephaly. *Brain Dev*. 1998;20:169-174.
10. Goutières F. Aicardi-Goutières syndrome. *Brain Dev*. 2005;27: 201-206.
11. Crow YJ, Leitch A, Hayward BE, et al. Mutations in genes encoding ribonuclease H2 subunits cause Aicardi-Goutières syndrome and mimic congenital viral brain infection. *Nat Genet*. 2006;38: 910-916.
12. Crow YJ, Hayward BE, Parmar R, et al. Mutations in the gene encoding the 3'-5' DNA exonuclease TREX1 cause Aicardi–Goutières syndrome at the AGS1 locus. *Nat Genet*. 2006;38: 917-920.
13. Rice GL, Bond J, Asipu A, et al. Mutations involved in Aicardi–Goutières syndrome implicate SAMHD1 as regulator of the innate immune response. *Nat Genet*. 2009;41:829-832.
14. Crow YJ, Black DN, Ali M, et al. Cree encephalitis is allelic with Aicardi-Goutières syndrome: implications for the pathogenesis of disorders of interferon alpha metabolism. *J Med Genet*. 2003;40: 183-187.
15. Sanchis A, Cerveró L, Bataller A, et al. Genetic syndromes mimic congenital infections. *J Pediatr*. 2005;146:701-705.
16. Burn J, Wickramasinghe HT, Harding B, Baraitser M. A syndrome with intracranial calcification and microcephaly in two sibs, resembling intrauterine infection. *Clin Genet*. 1986; 30:112-116.
17. Kalyanasundaram S, Dutta S, Narang A, Katariya S. Microcephaly with plate-like cortical calcification. *Brain Dev*. 2003;25: 130-132.
18. O'Driscoll MC, Daly SB, Urquhart JE, et al. Recessive mutations in the gene encoding the tight junction protein occludin cause band-like calcification with simplified gyration and polymicrogyria. *Am J Hum Genet*. 2010;87:354-364.
19. Weiss JL, Cleary-Goldman J, Tanji K, et al. Multicystic encephalomalacia after first-trimester intrauterine fetal death in monochorionic twins. *Am J Obstet Gynecl*. 2004;190: 563-565.

De Novo 5q14.3 Translocation 121.5-kb Upstream of *MEF2C* in a Patient With Severe Intellectual Disability and Early-Onset Epileptic Encephalopathy

Hirotomo Saitsu,[1]* Noboru Igarashi,[2] Mitsuhiro Kato,[3] Ippei Okada,[1] Tomoki Kosho,[4] Osamu Shimokawa,[5] Yuki Sasaki,[5] Kiyomi Nishiyama,[1] Yoshinori Tsurusaki,[1] Hiroshi Doi,[1] Noriko Miyake,[1] Naoki Harada,[5] Kiyoshi Hayasaka,[3] and Naomichi Matsumoto[1]

[1]Department of Human Genetics, Yokohama City University Graduate School of Medicine, Yokohama, Japan

[2]Department of Pediatrics, Toyama Prefectural Central Hospital, Toyama, Japan

[3]Department of Pediatrics, Yamagata University Faculty of Medicine, Yamagata, Japan

[4]Department of Medical Genetics, Shinshu University School of Medicine, Matsumoto, Japan

[5]Cytogenetic Testing Group B, Advanced Medical Science Research Center, Mitsubishi Chemical Medience Corporation, Nagasaki, Japan

Recent studies have shown that haploinsufficiency of *MEF2C* causes severe intellectual disability, epilepsy, hypotonia, and cerebral malformations. We report on a female patient with severe intellectual disability, early-onset epileptic encephalopathy, and hypoplastic corpus callosum, possessing a de novo balanced translocation, t(5;15)(q13.3;q26.1). The patient showed upward gazing and tonic seizure of lower extremities followed by generalized clonic seizures at 4 months of age. Electroencephalogram showed hypsarrhythmia when asleep. By using fluorescent in situ hybridization (FISH), southern hybridization and inverse PCR, the translocation breakpoints were determined at the nucleotide level. The 5q14.3 breakpoint was localized 121.5-kb upstream of *MEF2C*. The 15q26.2 breakpoint was mapped 119-kb downstream of *LOC91948* non-coding RNA. We speculate that the translocation may disrupt the proper regulation of *MEF2C* expression in the developing brain, resulting in severe intellectual disability and early-onset epileptic encephalopathy. © 2011 Wiley Periodicals, Inc.

Key words: *MEF2C*; early-onset epileptic encephalopathy; chromosomal translocation; regulatory region

INTRODUCTION

Early-onset epileptic encephalopathies, onset before 1 year of age, are characterized by severe seizures (often infantile spasms), frequent interictal epileptiform activity on a disorganized electro-encephalogram (EEG) background, developmental regression, or retardation [Holland and Hallinan, 2010]. Ohtahara syndrome (OS), West syndrome, early myoclonic epileptic encephalopathy (EME), migrating partial seizures of infancy, and Dravet syndrome are the most well-known epileptic encephalopathies recognized by the International League Against Epilepsy (ILAE). However, many infants with these disorders do not strictly fit into the electroclinical

How to Cite this Article:
Saitsu H, Igarashi N, Kato M, Okada I, Kosho T, Shimokawa O, Sasaki Y, Nishiyama K, Tsurusaki Y, Doi H, Miyake N, Harada N, Hayasaka K, Matsumoto N. 2011. De novo 5q14.3 translocation 121.5-kb upstream of *MEF2C* in a patient with severe intellectual disability and early-onset epileptic encephalopathy.

Am J Med Genet Part A 155:2879–2884.

parameters of these encephalopathies. Brain malformations and metabolic disorders were found as underlying causes of these syndromes, but a significant portion of idiopathic or cryptogenic cases remains etiologically unexplained. Recently, several causative genes have been reported: *ARX* in the OS and West syndrome phenotypes, *CDKL5* in West syndrome, *STXBP1* in OS, *SLC25A22*

2879

in EME, *SCN1A* in Dravet syndrome [Claes et al., 2001; Stromme et al., 2002; Kalscheuer et al., 2003; Molinari et al., 2005; Kato et al., 2007; Saitsu et al., 2008]. Identification of new causative genes is absolutely necessary for further understanding of infantile epileptic syndromes.

Microdeletions at 15q14.3 encompassing the *myocyte enhancer-binding factor 2C* (*MEF2C*) gene has been recently reported in patients with severe intellectual disability (ID), epilepsy often starting in infancy, hypotonia, and cerebral malformations [Cardoso et al., 2009; Engels et al., 2009; Le Meur et al., 2010]. Identification of five de novo mutations (three truncating and two missense ones) in *MEF2C* and a deletion only involving *MEF2C* in patients with similar phenotype clearly demonstrated that haploinsufficiency of *MEF2C* is responsible for these features [Le Meur et al., 2010; Novara et al., 2010; Nowakowska et al., 2010; Zweier et al., 2010]. Various kinds of seizures were observed in these patients with *MEF2C* abnormalities, including infantile spasm, and myoclonic, tonic-clonic, and febrile seizures [Le Meur et al., 2010; Novara et al., 2010; Nowakowska et al., 2010; Zweier et al., 2010]. Interstingly, a 3.57-Mb microdeletion 233.3-kb upstream of *MEF2C* resulted in significant loss of *MEF2C* expression in a patient with severe ID, hypotonia, epilepsy, and stereotypic hand movements [Zweier et al., 2010]. Moreover, a de novo balanced translocation, t(5;8)(q14.3;q23.3), in a patient with ID, epilepsy, and stereotypic movements has been reported, showing that the 5q14.3 breakpoint was located approximately 500-kb upstream of *MEF2C* [Floris et al., 2008]. All of these reports support the importance of upstream regulatory regions in controlling *MEF2C* expression.

Here, we report on a patient with severe intellectual disability and early-onset epileptic encephalopathy as well as a de novo balanced translocation, t(5;15)(q13.3;q26.1), which turned out related to *MEF2C*. Detailed genomic analysis is presented.

CLINICAL REPORT

The 7-year-old girl is a product of unrelated healthy parents. She was born at term without asphyxia after uneventful pregnancy. Body weight at birth was 2,584 g (−1.1 SD), height 47.0 cm (−1.0 SD), and head circumference 31.0 cm (−1.6 SD). Poor visual contact and nystagmus were noticed at 3 months of age. Ophthalmic examinations were unremarkable. Upward gazing and tonic seizures of lower extremities followed by generalized clonic seizures were observed at 3 months of age. EEG showed hypsarrhythmia when asleep (Fig. 1A). Seizures, which were observed as many as 40 times a day, were transiently controlled by combination of valproic acid, adrenocorticotropic hormone administration, and clobazam. Cerebral blood flow examination revealed low perfusion at right frontal area. Brain magnetic resonance imaging (MRI) showed reduced volume of white matter and normal cortical brain structure except for hypoplastic corpus callosum, especially in genu and splenium (Fig. 1B,C).

Profound intellectual disability and developmental delay ensued. The patient showed spastic quadriplegia, but no hypotonia. She could not walk or speak a word. Eye contact was poor. She could neither sit alone nor turnover, and required total care. She showed gastroesophageal refflux and was tube-fed. She did not exhibit stereotypic movements. The EEG at the age of 4 years showed

irregular high-voltage slow wave activity intermingled with fast wave. At present, her weight was 11.5 kg (−2.7 SD), height 108 cm (−2.5 SD), and head circumference 45.0 cm (−4.8 SD). She had severe deformity of trunk and extremities. Brief tonic seizures with blinking were observed several times a day despite administration of antiepilepstic drugs (valproic acid, clobazam, and zonisamide). In infancy, she had a square face with short palpebral fissures, a short and depressed nose with anteverted nostrils, a tented vermilion of the upper lip, and a protruded tongue. In childhood, her face became round and flat. The tented vermillion of upper lip might be shared by the patient and several patients with *MEF2C* abnormalities.

MATERIALS AND METHODS

### Molecular Cytogenetic Analysis

G-banded chromosomes of peripheral blood lymphocytes were analyzed. Fluorescence in situ hybridization (FISH) was performed on fixed peripheral lymphocytes. Labeling, hybridization, wash, and image acquisition were performed as previously described [Saitsu et al., 2008]. RPCI-11 BAC clones and approximately 15-kb probes amplified by long PCR using KOD-FX polymerase (Toyobo, Osaka, Japan) using RP11-634n8 DNA as a template were used as probes. Primer information is shown in the Supplemental eTable available online in Supporting Information.

Affymetrix Cytogenetics Whole-Genome 2.7M Array

Copy number alterations were studied by Cytogenetics Whole-Genome 2.7M Array (Affymetrix, Santa Clara, CA). Experimental procedures were performed according to the manufacturer's protocol. Copy number alterations were analyzed by Chromosome Analysis Suite (ChAS; Affymetrix) with NA30.1 (hg18) annotations.

Cloning of Translocation Breakpoints

The 5q14.3 translocation breakpoint was analyzed by Southern hybridization using *BglII*- and *SacI*-digested patient DNA. Mother's DNA was used as a control. Probes were synthesized by PCR DIG probe synthesis kit (Roche, Basel, Switzerland) using RP11-634n8 DNA as a template. Hybridization, washing, and detection of probes were done according to the manufacturer's protocol. Images were captured on FluorChem (Alpha Innotech, San Leandro, CA). To obtain the der(5) translocation junction fragment, *SacI*-digested DNA of the patient was self-ligated by Ligation high Ver.2 (Toyobo), ethanol precipitated and dissolved in 20 μl EB buffer (Qiagen, Tokyo, Japan). Inverse PCR was performed in 25 μl of volume, containing 2 μl ligated DNA, 1× PCR Buffer for KOD FX, 0.4 mM each dNTP, 0.3 μM each primer, and 0.3 U KOD FX polymerase (Toyobo). Negative controls only used either forward or reverse primer. The PCR product was electrophoresed in 0.7% agarose gel, and the aberrant band corresponding to der(5) fragment was purified by QIAquick Gel Extraction Kit (Qiagen). The purified DNA was sequenced for both forward and reverse
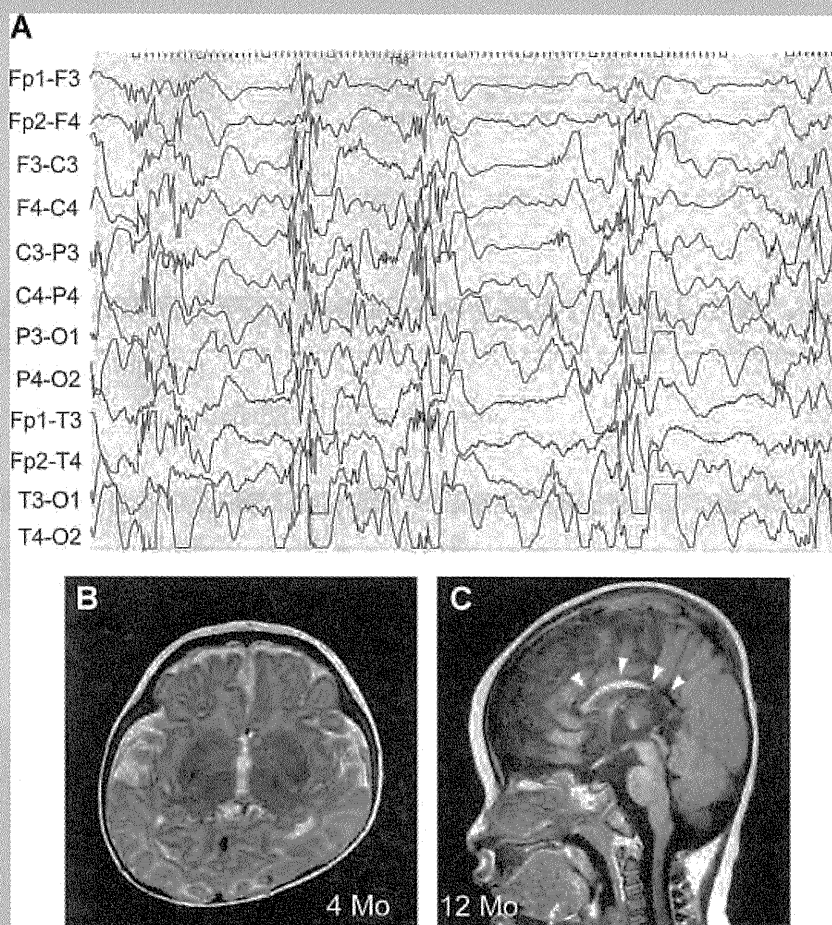
FIG. 1. EEG and brain MRI in the patient. A: Interictal sleep EEG at 4 months demonstrated diffuse or multifocal polyspikes or sharp waves concomitant with irregular high-voltage slow wave. Desynchronization lasting for 1–2 sec can also be seen predominantly in bilateral frontal area. B,C: Brain MRI of the patient at age of 4 months (B) and 12 months (C). T2-weighted axial (B) and T1-weighted sagittal (C) images showed normal cortical brain structure except for hypoplastic corpus callosum (arrowheads), especially in genu and splenium.

strands with BigDye Terminator chemistry ver. 3 according to the standard protocol (Applied Biosystems, Foster city, CA). After identification of breakpoint sequences of der(5), breakpoint-specific primers for both der(5) and der(15) translocation junctions were designed. Junction fragments were amplified by PCR using these primer-sets on DNAs of the patient and her parents. Primer information is shown in the Supplemental eTable available online in Supporting Information.

RESULTS

G-banded chromosomal analysis revealed a balanced translocation t(5;15)(q13.3;q26.1) (Fig. 2A). Her parents showed a normal karyotype (data not shown), indicating that the translocation occurred de novo. Subsequent FISH analysis demonstrated that the breakpoints in chromosome 5 and 15 were covered by the clones RP11-690g22 and 634n8, and 1061g3, respectively, indicating that the translocation did not directly disrupt any genes (Fig. 2B–D).

Interestingly, the breakpoint on 5q14.3 was located near the MEF2C gene, a causative gene for severe ID, epilepsy, and cerebral malformations [Cardoso et al., 2009; Engels et al., 2009; Le Meur et al., 2010; Novara et al., 2010; Nowakowska et al., 2010; Zweier et al., 2010]. The breakpoint on 5q14.3 was further narrowed down by FISH analysis using long PCR products as probes (Fig. 2C). Probe II showed weak but clear signals on chromosome 5, and derivative chromosomes 5 and 15, suggesting that the breakpoint was located within the probe II (data not shown). Southern hybridization analysis using probes P1 and P2 detected different aberrant bands only in the patient (Fig. 2C,E), indicating that the breakpoint was located at the region between the two probes. Inverse PCR on SacI-digested DNA was successful in obtaining a der(5) breakpoint-junction fragment. Sequence analysis showed that the 5q14.3 breakpoint was located 121.5-kb upstream of the transcription start site of MEF2C (isoform 1, NM_002397.3) (Fig. 2C,F). Breakpoint-specific PCR analysis of the patient and her parents confirmed that the rearrangements occurred de novo (Fig. 2G). The